A Faraday cup for charge measurements in biophysical and environmental fieldwork

Journal of Electrostatics 135 (2025) 104062

Contents lists available at ScienceDirect

Journal of Electrostatics

journal homepage: www.elsevier.com/locate/elstat

A Faraday cup for charge measurements in biophysical and environmental fieldwork

R. Giles Harrison [a,*], Daniel Robert [b]

[a] Department of Meteorology, University of Reading, UK
[b] School of Biological Sciences, University of Bristol, UK

A B S T R A C T

A novel miniature (28 mm × 38 mm) shielded Faraday cup is described for quantifying picocoulomb charges on millimetre environmental objects, such as small insects or plants, droplets, dust particles or powders. The electrometer electronics is contained within the device, avoiding any transfer of low level signals to an external electrometer. It is calibrated using a voltage ramp – capacitor method, generating defined charge pulses without a reference electrometer. The device can fit within an acoustic levitator to provide non-contact, zero leakage suspension of small objects, measuring charge on their release. Convenience and simplicity of use open new environmental charge measurement opportunities.

1. Introduction

Small electric charges at the picocoulomb (pC, 10^{-12}C) level occur on many natural materials, such as insects and plants, and fog droplets and dust particles. For example, the average charge on a bumble bee is 32 pC [1], and ~1 pC is carried by a millimetre snow particle [2]. Volcanic ash also readily acquires charge [3], and charging of Sahara dust has been suggested as a factor contributing to its unexpectedly long-range transport [4].

Measuring objects' charges in their natural environment requires a robust charge collection system which is easily deployed and facilitates rapid and straightforward measurement. Laboratory grade electrometers are unsuitable for this as they require mains power supplies and lack robustness and durability. The scientific need for such instrumentation, adapted to circumvent these practical constraints, has led to the development of the compact Faraday cup collector described here. A further application is in combination with ultrasonic levitation, to allow charge measurement following non-contact manipulation of a levitated, electrically isolated object [5].

This paper provides background on the operating principles in Section 2. The charge measuring device developed is described in Section 3 and evaluated in Section 4. Section 5 describes proof of concept tests deploying the Faraday cup within an ultrasonic levitator and Section 6 provides some conclusions about the use of the device.

2. Background and motivation

The Faraday cup is a charge collector commonly used in vacuum systems e.g. in space [6], and mass spectrometry [7], but the principle of charge collection using an isolated shaped conductor offers a general measurement method, including for granular materials [8]. A closely related device is the Faraday pail, which operates on the classical principle of induction [9], allowing an object's charge to be determined without it becoming discharged to the conductor into which it is inserted.

Modern use of a Faraday pail is described in Ref. [10]. This apparatus – the JCI141 Faraday pail - has previously been applied to laboratory studies of pollinators and their electrostatic interactions with flowers [1,11,12]. However, for environmental field work, the Chubb Faraday pail is cumbersome and lacks sensitivity at the pC level. Nevertheless, it has provided inspiration for this work, as its design draws on long experience in electrostatic instruments and measurements [13].

The miniature design of collector presented here is compact and portable, and therefore more suitable for field work and laboratory-based characterisation of millimetre-scale materials. Importantly, in this new system, the signal conditioning electronics is integrated within the collector itself, which offers an improved approach when sensitive measurements are required (see also Fig. 2a of [14]). In particular, the need for screened and rigid low level signal cables is avoided, which in turn reduces power line interference, and error currents generated by cable movement. To remove the requirement for a reference electrometer, which is an expensive laboratory item, the current amplifier's

* Corresponding author.
E-mail address: r.g.harrison@reading.ac.uk (R.G. Harrison).

https://doi.org/10.1016/j.elstat.2025.104062
Received 22 November 2024; Received in revised form 21 January 2025; Accepted 3 March 2025
Available online 11 March 2025

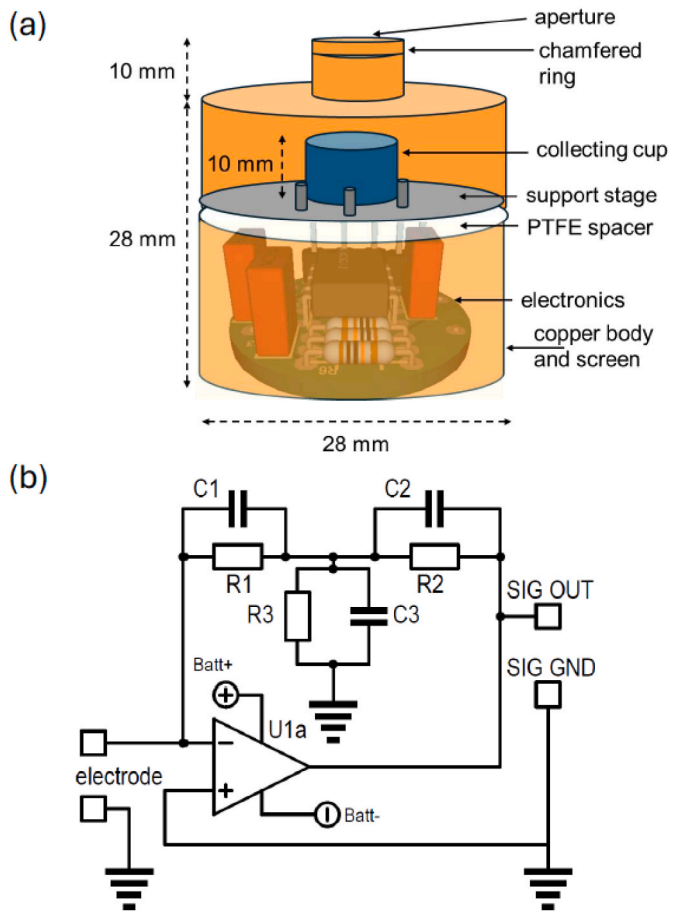

Fig. 1. (a) Arrangement of the integrated Faraday cup, showing the collecting cup electrode mounted within the outer copper body on a support stage. The electrometer electronics is mounted beneath the support stage. (b) Functional aspects of the electrometer circuit. The circuit is powered from a 5 V supply applied across Batt+ and Batt-, with the signal ground held at the mid-point of the battery supply. The output signal is measured between SIG OUT and SIG GND. (*Components*: U1 LMC6042, R1 1 GΩ ± 10 %, R2 10 MΩ, R3 150 kΩ, R C1 15 pF polystyrene, C2 220 pF, C3 100 nF).

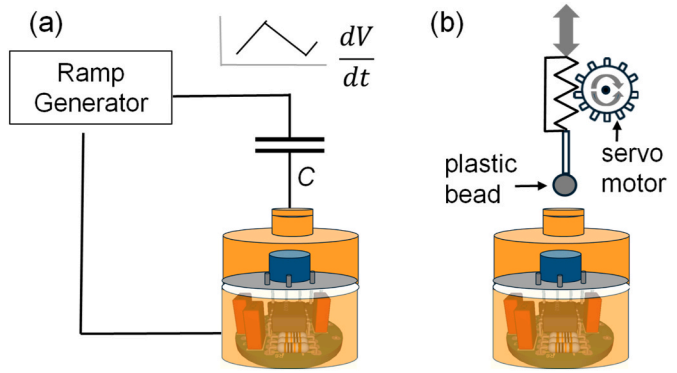

Fig. 2. Test configurations employed. (a) Charge collection. A steadily increasing and decreasing voltage ramp is applied through a polystyrene capacitor to the cup electrode, to provide a known current. (b) Induction. A charged bead is regularly inserted and withdrawn by a servo motor, without the bead touching the electrode.

response has been characterised using a range of known currents generated using a voltage ramp and capacitor method.

A particular feature of the Chubb design of Faraday pail is its narrow entrance to maximise screening of the inner pail, with rounded surfaces around the opening. A similar approach has been adopted in the miniature Faraday cup device, which has been designed to fit physically within the TinyLev ultrasonic levitator [15] to further broaden the range of charge measurement applications.

3. Description

The Faraday cup arrangement is cylindrical, 28 mm in diameter and 38 mm high, constructed from turned copper (see Fig. 1a). A chamfered cap is fitted on top of the outer housing, having a small central sampling opening emulating the top of the Chubb pail, designed to provide maximum screening from external sources of noise. The collecting cup electrode is mounted on an aluminium disk support stage, fitted with vertical pegs to hold the copper measuring cup in place. This clamping arrangement also provides a convenient way to quickly substitute one measuring cup for another, for example to allow drying following collection of a liquid drop, or for the retrieval of an individual particle. The support stage sits on a 1 mm thick PTFE insulator, through which a wired connection is made to the signal conditioning electronics beneath.

This electrometer circuitry is housed beneath the support stage, and converts the small currents induced or supplied to the cup, to voltages measured by a separate device. The entire assembly is enclosed within the outer copper housing, which is connected to the local ground and provides shielding. Items to be measured are brought into the top of the copper cylinder and placed within the collecting cup electrode. Although all the circuitry is contained within the device, the chamfered cap acts to screen the collecting electrode area as much as possible from power line and other external sources of interference. The output from the electrometer electronics is a driven high-level signal, allowing it to be used with long and/or flexible signal cables as necessary.

There are several possible options for the electrometer. The charge collected can in principle be found using (1) a voltage measurement, (2) a charge amplifier or (3) a current measurement, the latter integrated over the charge-delivery duration to provide the total charge. Whilst approach (1) is simplest and is implemented by non-contact voltage sensing in the Chubb Faraday pail, the system capacitance required is a difficult quantity to determine for a small device as stray capacitances can be significant. Approach (2) would require reset circuitry to be implemented (e.g. using a reed switch or guarded mosfet switch), introducing additional parts for a device intended to fit in a small volume. These considerations led to the implementation of the third approach, which offers relative simplicity. An electrometer current amplifier with a nominal magnitude response of 100 mV/pA was designed, for measuring particles or fragments of insects carrying charges in the range 0.1 pC–10 pC, notionally released into the collector in 1 s (i.e. yielding a short output pulse of 10 mV–1000 mV).

Fig. 1b provides a schematic showing the principal aspects of the electrometer current amplifier. For the prototype version, this was constructed with through-hole components, on a circular circuit board. The circuit consists of an electrometer current-to-voltage converter, based around operational amplifier U1a, which is a type selected to have a low bias current i_b, at the fA level. This is a conventional trans-resistance configuration, but with a "T network" in its resistive feedback loop. A T-network allows a large effective feedback resistance to be synthesised from a smaller feedback resistance R_1. The effective feedback resistance R_f is increased above R_1 by the ratio [16] of R_2 to R_3, as

$$R_f = R_1\left[1+\frac{R_2}{R_3}\right] \tag{1}$$

a result which is derived in the Appendix. The overall response of the electrometer circuit is to provide an output voltage V_e, according to

$$V_e = -(i+i_b)R_f \tag{2}$$

where i is the input current, and $i \gg i_b$. (The polarity inversion arises due

to the input current being applied to the opamp's inverting input.)

In the feedback network, the stray capacitance of R_1 will act to roll-off the time response. A larger capacitance swamping the stray capacitance is provided by adding capacitor C_1, in parallel with R_1. The combination of R_3 and C_3 acts to compensate the roll-off of gain with frequency of R_1 by C_1, their values chosen to match the time constants (i.e. $R_1C_1 \approx R_3C_3$). C_2 in parallel with R_2 acts to reduce any initial ringing which can occur with transient current pulses. One disadvantage of the T-network approach is that the opamp's offset voltage is also amplified by $\approx R_2/R_3$. However, in this application, since only changes are typically being observed rather than steady currents, this is relatively unimportant. Overall, the key advantages provided by the T-network are the ability to use physically small resistors in the feedback circuit, and to allow the time response to be improved compared with a single large value resistor.

To allow operation from a single battery, a local signal ground is generated from the centre voltage of the battery supply. This local ground is applied to the body of the Faraday cup and provides the reference against which the signal output is measured. A disadvantage of the split battery supply is that the output signal is referenced to the mid-supply ground (rather than battery negative), e.g. nominally at 2.5 V when the system is powered from 5 V using a USB power bank. Measuring the final output therefore either requires the use of a floating voltmeter, or two analogue inputs which are ground referenced and their values subsequently differenced. Alternatively, it can be assumed that the signal ground has a fixed value, which is then subtracted from the signal output.

4. Evaluation

Two different methods are used to evaluate the operation of the system, using the response to (1) finite currents from which the charge could be derived, and (2) induced charge. Fig. 2 summarises these methodologies.

(a) Methodology

In the first approach a range of reference currents were produced, typical of those likely to be generated by the anticipated measurements. Known input currents around 10^{-12} A can be generated by the voltage ramp method, supplying a steadily increasing or decreasing voltage through a known value capacitor to a sensing node [17]. This general approach has since seen increasing use in standards laboratories [18].

To apply this method, a low leakage capacitor is connected between a voltage ramp generator and the Faraday cup, Fig. 2a. After a short settling time, a steady current is generated as the ramp voltage rises or falls at a constant rate. The current is found from the voltage ramp rate dV/dt and the capacitor C as

$$i = C\frac{dV}{dt} \tag{3}$$

By varying the voltage ramp rate dV/dt, a range of input currents can be generated. The voltage ramp was generated using an Arduino microcontroller system interfaced with a 12-bit digital to analogue converter (DAC, type MCP4822). This arrangement was programmed to generate a steadily increasing and decreasing voltage around the local ground voltage, repeating indefinitely. As the voltage ramp rate is controlled in software and the DAC voltage has 12-bit accuracy, the calibration current generated is dependent primarily on the capacitor, which will be known to a specified uncertainty (e.g. ±5 % or ±1 %).

In the second case, the operation by electrostatic induction is evaluated. This was achieved by moving a charged nylon bead in and out of the Faraday cup, using a servo motor operating a rack and pinion system to provide a linear displacement (Fig. 2b). The servo motor was controlled by a further Arduino microcontroller, allowing intervals between the insertion and withdrawal to be programmed, together with the rate of motion in either case.

These two approaches allow the response of the system to known currents to be evaluated and to confirm the response to an induced charge.

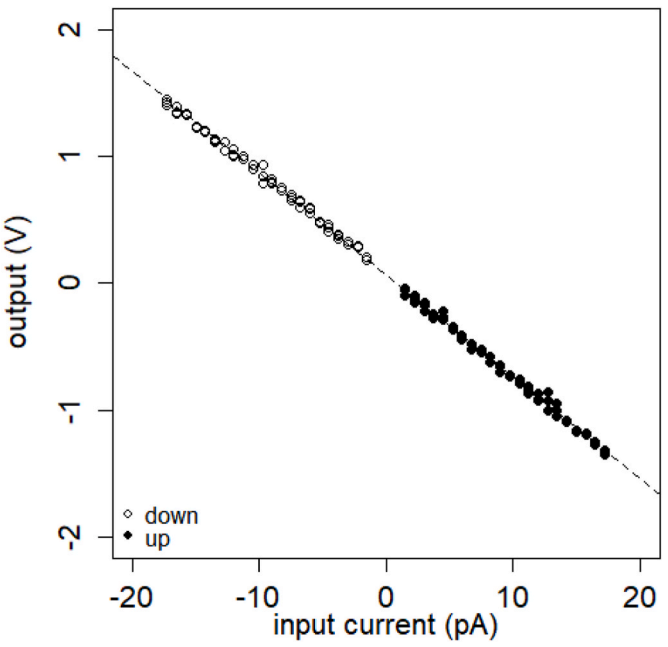

Fig. 3. Current supplied by the ramp voltage method plotted against the output voltage (found as SIGOUT - SIGGND), for a range of different voltage ramp rates both increasing (solid points) and decreasing (hollow points). The line's gradient is – (80.1 ± 0.3) mV per pA, and the zero offset (65.5 ± 3) mV, with the uncertainties in the fit given as one standard error.

(b) Results

Fig. 3 shows results from the voltage ramp method of Fig. 2a, with slowly increasing and decreasing voltage ramps generated by the Arduino and DAC combination. The rising and falling ramp voltages were supplied to the Faraday cup through a 15 pF polystyrene capacitor. DC leakage through the capacitor was minimised by the capacitor having a high resistance dielectric (polystyrene), and by operating the ramp generated at close to the mid-point voltage of the supply (and therefore at the virtual earth of the opamp's input), to ensure the voltage difference across the capacitor is minimised.

The output voltages from the Faraday cup were also recorded by the same Arduino microcontroller, using its analogue to digital converter (ADC). A linear response is evident between the output voltage and the input current, over a range of 0 to ±20 pA. From equations (1) and (2), the expected response would be −68 mV per pA, should the components in Fig. 1b have their precise values. The actual measured sensitivity was −80 mV per pA of input current, i.e. ~15 % greater than the calculated value. Although no accurately defined response was sought, the combination of several component and measurement uncertainties mostly account for this difference: R1 (±10 %), R2, R3 (±5 %), calibration capacitor (±5 %) and the ADC reference voltage (±5 %). Stray capacitance may also have contributed to the ramp capacitor's value.

If a long duration voltage ramp is replaced by a voltage ramp of a fixed, short duration, the charge delivered to the Faraday cup can be controlled. The charge Δq is given by

$$\Delta q = C\frac{dV}{dt}T \tag{4}$$

where T is the duration for which the voltage ramp occurs. In principle, both T and dV/dt can be varied, to vary Δq. However, it is convenient to

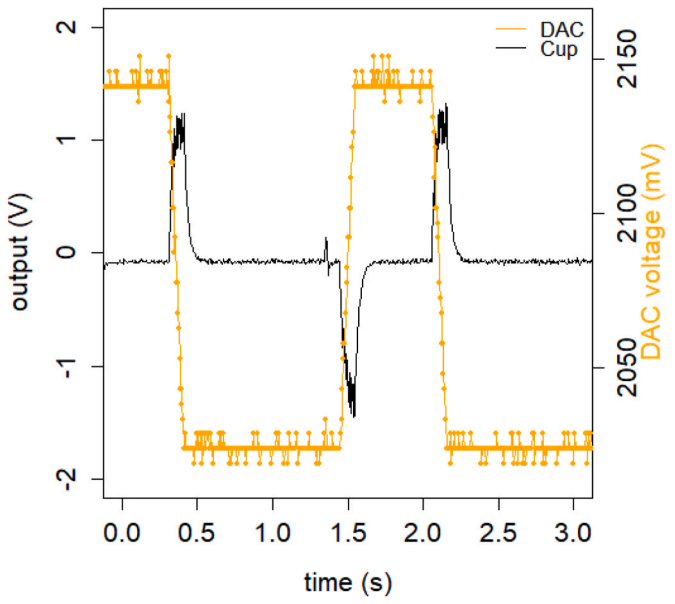

Fig. 4. Example of the transient response to short duration voltage increases and decreases. The orange trace (right-hand axis) shows the voltage ramp generated by the DAC, delivered to the cup through a 15 pF capacitor; the black trace is the electrometer response (left-hand axis). (For interpretation of the references to colour in this figure legend, the reader is referred to the Web version of this article.)

choose T to be comparable with the charge delivery time and kept constant: the slope of the voltage ramp dV/dt is then changed to vary the charge supplied. During the charge pulse, when the ramp voltage is steady, the instantaneous response of the current amplifier is given by equations (2) and (4) as

$$V_e = -\frac{\Delta q}{T} R_f \tag{5}$$

although the actual response in practice will also be influenced by the time response of the electrometer.

Fig. 4 shows the effect of introducing a short pulse of charge to the Faraday cup, to simulate an object being dropped into it. This was achieved by programming the Arduino and DAC combination to provide a short ramp voltage pulse, with a duration T of 100 ms (orange trace). The second trace on Fig. 4 shows the response from the Faraday cup. As expected from equation (5), there is an inverted response, with a positive-going output pulse associated with a decreasing Δq and negative-going pulse with increasing Δq.

Fig. 5 shows the effect of a short and steady voltage ramp, delivered to the electrometer via a small value (15 pF) polystyrene capacitor. The ramp trends upwards (Fig. 5a) and downwards (Fig. 5c): the associated electrometer responses are given in Fig. 5b and d respectively.

By integrating the electrometer determined current i_e with time t, the total charge received during application of the voltage ramp can be found. The charge found from the electrometer current is expected to be related to the current supplied by the voltage ramp $\frac{dV}{dt}$ and capacitor C, as

$$\int_0^T i_e(t)\, dt = k\, C \frac{dV}{dt} T \tag{6}$$

where k is a constant and T is the duration of the voltage ramp.

The associated charges determined from Fig. 5 examples are provided in Table 1, calculated for $T = 90$ ms and $C = 15$ pF. i_e is found from the electrometer voltage using the calibration from Fig. 3.

Fig. 5e shows charge responses derived in the same way for short duration (90 ms) voltage ramps, swept over a wide range of values. Although there are limitations due to the resolution of the

Table 1
Delivered and measured charges.

Voltage ramp direction	Measured rate of change $\frac{dV}{dt}$	Charge delivered $C\frac{dV}{dt}T$	Integrated electrometer output $\int_0^T i_e(t)\, dt$
Upwards (Fig. 5a)	547 (mV s^{-1})	0.74 pC	0.53 pC
Downwards (Fig. 5d)	−540 (mV s^{-1})	−0.73 pC	−0.53 pC

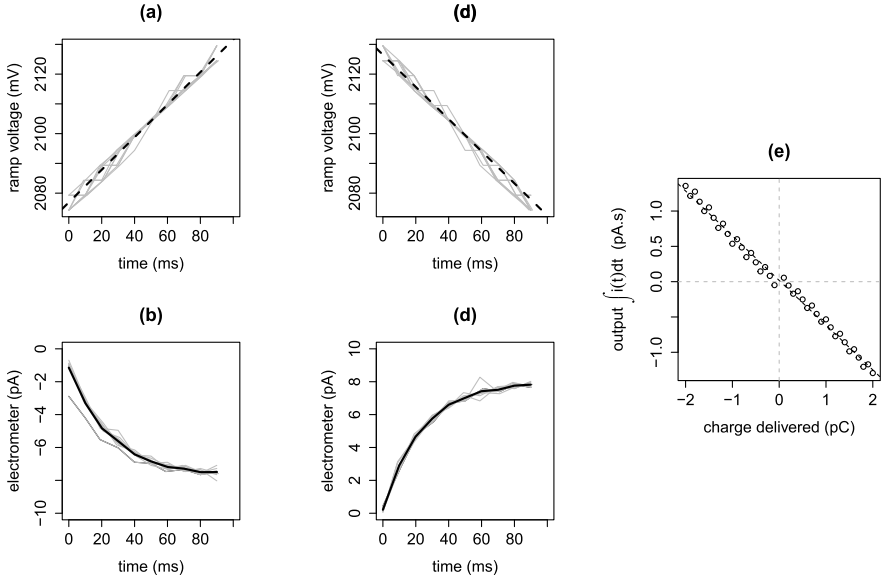

Fig. 5. Response to short duration voltage ramps. (a) and (c) give examples of the voltage ramps with (b) and (d) the associated electrometer responses. Integration with time of the current in (b) and (d) provides the total measured charge for the two cases. (e) shows a range of such events for different voltage ramp rates, with the measured currents integrated to give the charge, yielding a range of delivered charges. (In (a) and (d) the thin grey lines are from repeated voltage ramp experiments, with the dashed black lines found from least squares regression to the combined points; in (b) and (d) the thick black lines are the mean of the multiple realisations shown by the thin grey lines).

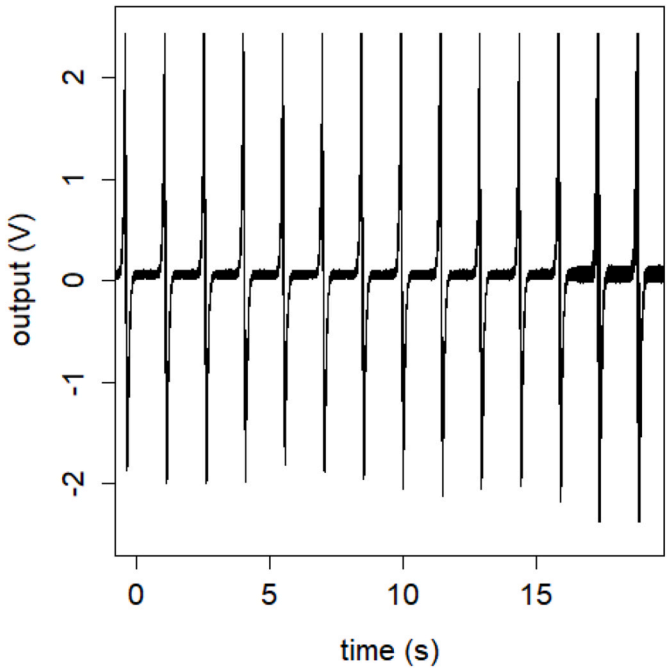

Fig. 6. Response of the device to a charged bead which is regularly inserted and withdrawn from the Faraday cup. (The positive-going output occurs as the bead is moved towards the cup, and a negative-going output as the bead is removed.)

measurements, the available ramp rates, and asymmetry in the opamp response between positive and negative inputs, a linear relationship is obtained over a range of charges, as expected from equation (6). The reduction in the measured charges compared with the delivered charges results from the finite response time of the electrometer: for longer duration pulses this effect would be proportionately less.

Fig. 6 shows the effect of introducing an electrostatically charged bead into the Faraday cup, without allowing the bead to touch the surface of the measuring cup. The movement associated with the servo was measured by a laser rangefinder as about 15 mm, with the displacement occurring in about 250 ms. As the bead is pushed into the cup a positive-going output pulse is generated. This positive pulse results from an induced negative charge, which is generated by a positively charged object. Interestingly, the charged bead is seen to approximately maintain its charge over multiple insertion-removal cycles (Fig. 6).

5. Levitation experiments

An intended new application of the Faraday cup is for measuring the charge on levitated objects, for example in assessing whether their charge is generated internally more rapidly than it is dissipated through the conductivity of the nearby air. Acoustic levitation is well suited to such investigations, as it ensures that the suspended object remains electrically isolated throughout any experiments. When the acoustic levitation is removed, the object falls into the Faraday cup beneath, allowing the remaining charge on it to be measured.

Fig. 7 shows the arrangement employed, using the Faraday cup within a TinyLev device, mounted in the centre of the lower set of acoustic transducers (Fig. 7a). The presence of the Faraday cup had only a small effect on the generated acoustic field, and did not prevent the levitation of small particles. The apparatus was arranged in a laboratory

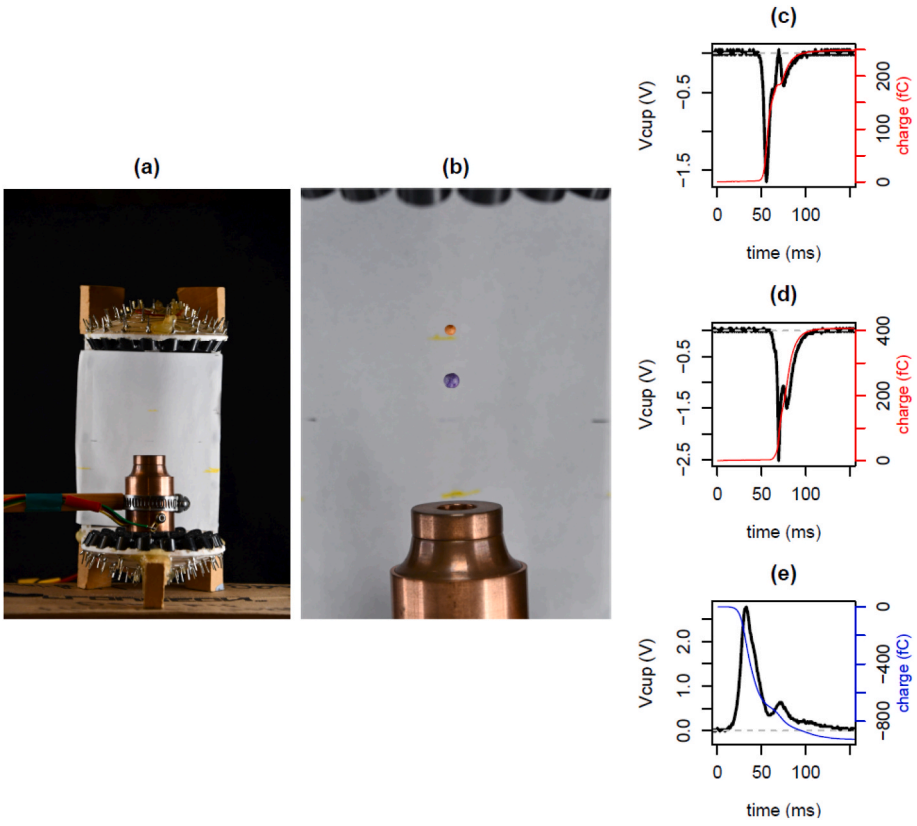

Fig. 7. Use of the Faraday cup to determine the charge on objects levitated with ultrasound. (a) TinyLev levitator with Faraday cup placed over the lower set of ultrasonic transducers. (b) A pair of polystyrene spheres of different diameters levitated at acoustic notes in the TinyLev. Current pulses at the Faraday cup for (c) and (d) freely charging polystyrene sphere after the acoustic levitation was switched off, and (e) after exposing a levitated sphere to a stream of negative ions. Coloured lines in (c), (d) and (e) provide the total charge, derived from time integration of the current pulse.

environment with low electrical noise. Fig. 7b shows the situation with two small polystyrene spheres levitated above the Faraday cup. After the levitation was switched off, current pulses were evident at the Faraday cup as the charged spheres fell into it. Fig. 7c and d shows the pulses produced by dropping two levitated spheres which were evidently charged. Using the fit derived in Fig. 3, the integrated charge received by the Faraday cup electrometer has been derived from the current pulse, and this is also shown in Fig. 7c and d. Fig. 7e shows the response for a polystyrene sphere exposed to unipolar ions during its levitation, emitted from an ion gun. The integrated charge in this case has a different polarity to that of Fig. 7c and d, demonstrating that, compared with charging freely, exposure to the ion gun allows the charge to be modified during the levitation.

6. Conclusions

These results show that the miniature Faraday cup electrode and electrometer systems behave consistently to charged items, at the picocoulomb level. When combined with an ultrasonic levitator, the charge on an object can be modified during levitation, and then determined by release into the Faraday cup. Overall, this compact and portable system opens a new range of experimental opportunities for biophysical and environmental charge measurements on small objects under real world conditions.

CRediT authorship contribution statement

R. Giles Harrison: Writing – review & editing, Writing – original draft, Methodology, Data curation, Conceptualization. **Daniel Robert:** Writing – review & editing, Investigation, Conceptualization.

Data availability

The data used in generating the figures in this paper, together with Arduino code and wiring schematics are available at https://doi.org/10.6084/m9.figshare.27680130. The ramp generator used is described at https://doi.org/10.6084/m9.figshare.28498094.

Declaration of competing interest

The authors declare that they have no known competing financial interests or personal relationships that could have appeared to influence the work reported in this paper.

Acknowledgements

Prof Chris Scott provided comments on the manuscript. Ultrasonic levitation for charged droplet measurements was initially investigated by Dr Martin Airey, under Science and Technology Facilities Council grant number ST/R000921/1.

Appendix. Equivalent T-network resistance in a trans-resistance amplifier

In a conventional trans-resistance amplifier with opamp U1 and single feedback resistor R (figure A1a), the opamp's entire output voltage v_0 appears across R, generating an equal and opposite current to the measurement current, which sums to zero at the inverting input. The input current i is therefore related to the output voltage by $v_0 = -iR$. With a T-network (figure A1b), the effective feedback resistance is found by considering the reduced voltage v_0' which is provided to R1, due to the combination of R1, R2 and R3.

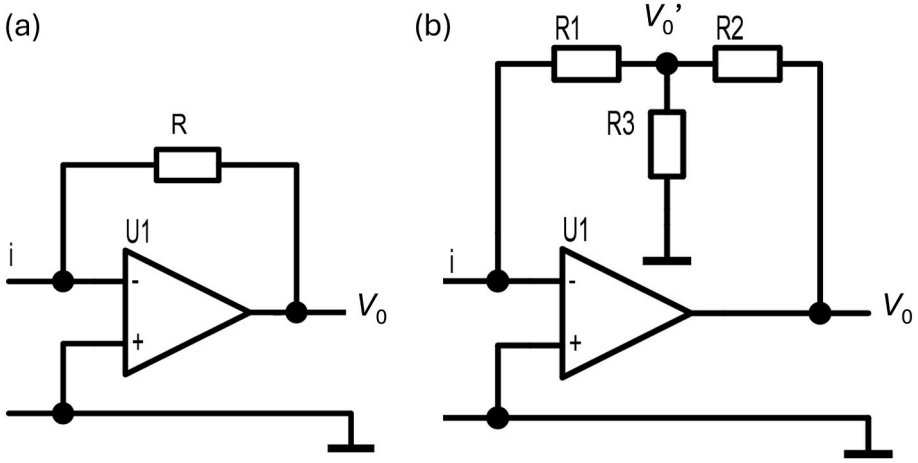

Fig. A1. Trans-resistance amplifiers with (a) a feedback resistor R and (b) a T-network of three resistors R1, R2 and R3 in the feedback path.

Assuming negligible offset voltage, the inverting input of U1 will be at virtual ground, with the lower end of R3 also at ground potential. The voltage v_0' at the junction of the three resistors is therefore equivalent to that of a potential divider consisting of R2 in the upper portion, with the lower portion the parallel resistance of R1-R3 to ground. The lower portion parallel resistance of R1 and R3 is given by

$$\left[\frac{1}{R_1}+\frac{1}{R_3}\right]^{-1}=\frac{R_1R_3}{(R_1+R_3)} \tag{A1}$$

and hence the potential divider voltage v_0' is

$$v_0'=v_0\left[\frac{\frac{R_1R_3}{(R_1+R_3)}}{\left\{\frac{R_1R_3}{(R_1+R_3)}+R_2\right\}}\right]=\left[\frac{\frac{R_1R_3}{(R_1+R_3)}}{\left\{\frac{R_1R_3}{(R_1+R_3)}+\frac{R_2(R_1+R_3)}{(R_1+R_3)}\right\}}\right]=\frac{R_1R_3}{(R_1R_3+R_2(R_1+R_3))} \tag{A2}$$

The measurement and feedback current flowing to the inverting input sums to zero, i.e., assuming negligible input bias current, the condition required is

$$i + \frac{v_0'}{R_1} = 0 \tag{A3}$$

and therefore

$$i + \frac{v_0}{R_1}\frac{R_1R_3}{(R_1R_3 + R_2(R_1 + R_3))} = 0 \tag{A4}$$

giving

$$v_0 = -iR_1\left[\frac{(R_1R_3 + R_2(R_1 + R_3))}{R_1R_3}\right] \tag{A5}$$

For $R_3 \ll R_1$, equation (A5) can be approximated by

$$v_0 = -iR_1\left[1 + \frac{R_2}{R_3}\right] \tag{A6}$$

and hence the effective feedback resistance R_f is

$$R_f = R_1\left[1 + \frac{R_2}{R_3}\right] \tag{A7}$$

References

[1] D. Clarke, H. Whitney, G. Sutton, D. Robert, Detection and learning of floral electric fields by bumblebees, Science 340 (6128) (1979), https://doi.org/10.1126/science.1230883, 2013.

[2] S. Omiya, A. Sato, K. Kosugi, S. Mochizuki, Estimation of the electrostatic charge of individual blowing-snow particles by wind tunnel experiment, Ann. Glaciol. 52 (58) (2011), https://doi.org/10.3189/172756411797252167.

[3] I.M.P. Houghton, K.L. Aplin, K.A. Nicoll, Triboelectric charging of volcanic ash from the 2011 Grímsvötn eruption, Phys. Rev. Lett. 111 (11) (2013), https://doi.org/10.1103/PhysRevLett.111.118501.

[4] M. van der Does, P. Knippertz, P. Zschenderlein, R.G. Harrison, J.B.W. Stuut, The mysterious long-range transport of giant mineral dust particles, Sci. Adv. 4 (12) (2018), https://doi.org/10.1126/sciadv.aau2768.

[5] M.W. Airey, R.G. Harrison, K.L. Aplin, C. Pfrang, B. McGinness, Electrical effects on droplet behaviour, in: Journal of Physics: Conference Series, 2024, https://doi.org/10.1088/1742-6596/2702/1/012015.

[6] H.S. Bridge, et al., The plasma experiment on the 1977 Voyager Mission, Space Sci. Rev. 21 (3) (1977), https://doi.org/10.1007/BF00211542.

[7] D.C. Imrie, J.M. Pentney, J.S. Cottrell, A Faraday cup detector for high-mass ions in matrix-assisted laser desorption/ionization time-of-flight mass spectrometry, Rapid Commun. Mass Spectrom. 9 (13) (1995), https://doi.org/10.1002/rcm.1290091314.

[8] T.F. O'Hara, D.P. Reid, G.L. Marsden, K.L. Aplin, Faraday cup measurements of triboelectrically charged granular material: a modular interpretation methodology, Soft Matter (2024), https://doi.org/10.1039/D4SM01124D [Online]. Available:. (Accessed 13 January 2025).

[9] M. Faraday, " XXXII. On static electrical inductive action ,", London, Edinburgh Dublin Phil. Mag. J. Sci. 22 (144) (1843) https://doi.org/10.1080/14786444308636351.

[10] J.N. Chubb, Measurement of charge transfer in electrostatic discharges, J. Electrost. 64 (5) (2006), https://doi.org/10.1016/j.elstat.2005.08.003.

[11] S.J. England, D. Robert, Electrostatic pollination by butterflies and moths, J. R. Soc. Interface 21 (216) (2024) 20240156, https://doi.org/10.1098/rsif.2024.0156.

[12] C. Montgomery, et al., Bumblebee electric charge stimulates floral volatile emissions in Petunia integrifolia but not in Antirrhinum majus, Sci. Nat. 108 (5) (2021), https://doi.org/10.1007/s00114-021-01740-2.

[13] P. Holdstock, Obituary -John Norman Chubb, The Guardian (19 Jan 2016) [Online]. Available: https://www.theguardian.com/science/2016/jan/19/john-chubb-obituary. (Accessed 23 August 2024).

[14] R.G. Harrison, Measuring electrical properties of the lower troposphere using enhanced meteorological radiosondes, Geoscientific Instrumentation, Methods and Data Systems 11 (1) (Jan. 2022) 37–57, https://doi.org/10.5194/gi-11-37-2022.

[15] A. Marzo, A. Barnes, B.W. Drinkwater, TinyLev: a multi-emitter single-axis acoustic levitator, Rev. Sci. Instrum. 88 (8) (2017), https://doi.org/10.1063/1.4989995.

[16] P. Horowitz, W. Hill, The Art of Electronics, third ed., Cambridge University Press, 2015.

[17] R.G. Harrison, K.L. Aplin, Femtoampere current reference stable over atmospheric temperatures, Rev. Sci. Instrum. 71 (8) (2000), https://doi.org/10.1063/1.1304859.

[18] S.P. Giblin, J. Tompkins, From counting electrons to calibrating ammeters: improved methodologies for traceable measurements of small electric currents, ArXiv (2020) 12669, 2003[Online]. Available: https://arxiv.org/pdf/2003.12669. (Accessed 19 November 2024).